ACS Award Address in Inorganic Chemistry

Electrides: From 1D Heisenberg Chains to 2D Pseudo-Metals†

James L. Dye

Department of Chemistry and Center for Fundamental Materials Research, Michigan State University, East Lansing, Michigan 48824

Received May 9, 1997[⊗]

Electrides are ionic compounds in which the cations are complexed by cryptands or crown ethers and the "anions" are trapped electrons. The crystal structures of five electrides are known and are similar to the corresponding alkalides (in which the anions are alkali metal anions) except that the anionic sites are "empty". Theory and experiment strongly support a model in which the "excess" electrons are trapped in these anionic cavities and interact with each other through connecting channels, whose geometries vary significantly from one electride to another. Measurements of optical, alkali metal NMR, and EPR spectra, magnetic susceptibilities, and conductivities provide many data that can be correlated with the structures. Three electrides have essentially 1D chains of cavities connected by channels through which the electrons communicate, as indicated by magnetic susceptibilities that are well described by a 1D Heisenberg model. The electride, K^+(cryptand[2.2.2])e^- has a 2D array of cavities and channels. It appears that defects, probably missing electrons (holes), are responsible for its near-metallic conductivity. The fifth electride of known structure contains Cs^+ complexed by a mixed sandwich of 15-crown-5 and 18-crown-6 and has a complex cavity−channel geometry, dominated by rings of six cavities. The arguments in favor of the proposed electride model, nearly-free electrons confined as a "lattice gas" in a complex array of cavities and channels, are presented in this paper.

Introduction

Solvated electrons[1] and electrons trapped at anion vacancies in alkali halide salts (F-centers)[2] have been known for over a century. In both cases the electron density is spread over a rather large, nearly spherical cavity rather than being confined to a particular atom or molecule. But the distance between these "excess" electrons is generally too great to provide extended interelectron interactions. At the other extreme are nearly-free-electron (NFE) metals, such as the alkali metals, in which interelectron effects are so strong that a nearly completely delocalized band picture is appropriate.[3] The compounds we call *electrides* are essentially *stoichiometric* F-center salts in which *all* anions are replaced by trapped electrons.[4] The keys to such materials are *large nonreducible* countercations that form substantial void spaces (cavities) when packed together[5,6] and that can coexist with the highly reducing trapped electrons. So far, the only cations that qualify are alkali metal cations trapped in cryptands[7−9] or sandwiched between crown ether molecules.[10,11]

The counterparts to electrides are *alkalides*, crystalline compounds with the same type of complexed cations, in which *alkali metal anions* occupy the anionic sites.[12,13] More than 35 such compounds that contain the anions Na^-, K^-, Rb^-, or Cs^- have been synthesized in our laboratory, and their crystal structures have been determined.[5,14,15] (Note the absence of Li^- salts.) In a sense, the trapped electron could be viewed as the simplest possible anion, but there is a significant difference between alkalides and electrides. Whereas the large alkali metal anions are confined to the cavities, only the probability density of trapped electrons can be defined. Electron density will pile up in regions of lowest total energy (potential plus kinetic), but the electronic wave function can extend into all regions of space, subject of course to orthogonality to core electrons and the Pauli exclusion principle.

A major advance in the past few years has been the realization that electron density tends to avoid the regions occupied by the

† This paper is based largely on the address for the 1997 ACS Award in Inorganic Chemistry presented as INOR 423 at the 213th National Meeting of the American Chemical Society, San Francisco, CA, April 15, 1997.

⊗ Abstract published in *Advance ACS Abstracts,* July 1, 1997.

(1) Thompson, J. C. *Electrons in Liquid Ammonia*; Oxford Univ. Press: Oxford, U.K., 1976; 297 pp.
(2) Markham, J. J. *F Centers in Alkali Halides*; Academic Press: New York, 1966; 400 pp.
(3) Kittel, C. *Introduction to Solid State Physics*, 6th ed.; John Wiley & Sons: New York, 1986; 646 pp.
(4) Dye, J. L. *Nature* **1993**, *365*, 10−11.
(5) Wagner, M. J.; Dye, J. L. In *Molecular Recognition: Receptors for Cationic Guests*, 1st ed.; Gokel, G. W., Ed.; Pergamon Press, Ltd.: Oxford, U.K., 1996; Vol. 1, pp 477−510.
(6) Dye, J. L.; Wagner, M. J.; Overney, G.; Huang, R. H.; Nagy, T. F.; Tomanek, D. *J. Am. Chem. Soc.* **1996**, *118*, 7329−7336.
(7) Dietrich, B.; Lehn, J.-M.; Sauvage, J. P. *Tetrahedron Lett.* **1969**, 2885−2888.
(8) Lehn, J.-M. *Struct. Bonding (Berlin)* **1973**, *16*, 1−70.
(9) Lehn, J.-M. In *Supramolecular Chemistry*; VCH: Weinheim, Germany, 1995; 271 pp.
(10) Pedersen, C. J. *J. Am. Chem. Soc.* **1967**, *89*, 2495−2496.
(11) Pedersen, C. J. *J. Am. Chem. Soc.* **1967**, *89*, 7017−7036.
(12) Dye, J. L.; Ceraso, J. M.; Lok, M. T.; Barnett, B. L.; Tehan, F. J. *J. Am. Chem. Soc.* **1974**, *96*, 608−609.
(13) Tehan, F. J.; Barnett, B. L.; Dye, J. L. *J. Am. Chem. Soc.* **1974**, *96*, 7203−7208.
(14) Dye, J. L. In *Metals in Solution, Journal de Physique IV, Colloque C5*; Damay, P., Leclerq, F., Eds.; Les Editions de Physique: Les Ulis, France, 1991; Vol. 1, pp 259−282.
(15) Dye, J. L. *Chemtracts: Inorg. Chem.* **1993**, *5*, 243−270.

S0020-1669(97)00551-X CCC: $14.00

James L. Dye was born in Soudan, MN, in 1927. After graduation from Gustavus Adolphus College in 1949, he began Ph.D. research on lanthanide separation and electrochemistry with Frank H. Spedding at Iowa State University. Upon completion of this degree in 1953, Dye began a 44 year research and teaching career at Michigan State University. During his first year, a graduate student seminar about the metal−ammonia research of Charles A. Kraus inspired him to begin research on solvated and trapped electrons, a passion that continues to this day. His experience was broadened by five sabbatical leaves with Manfred Eigen in Göttingen, Germany (NSF Science Faculty Fellowship, 1961−2); Leon Dorfman at The Ohio State University, 1968−9; Jean-Marie Lehn in Strasbourg, France (Fulbright and Guggenheim, 1975−6); Donald Murphy and Andrea Wayda at Bell Labs, 1982−3; and Frank Di Salvo at Cornell (Guggenheim, 1990−1). A watershed in his research came in 1970 with the use of crown ethers and cryptands to enhance alkali metal solubilities in amines and ethers. This led to the isolation in 1974 of the first salt of an alkali metal anion (alkalide) and in 1983 to the first crystalline electride. Dye is a member of the National Academy of Sciences and the American Academy of Arts and Sciences. Since his formal retirement in 1994, he has continued research under NSF and AFOSR Grants, with time off for fishing, golf, and visiting children and grandchildren.

closed-shell complexant molecules and the cations and to seek out the void spaces provided by the cavities and by intercavity channels.[4,6,16] This behavior is so pronounced that, to first order, we may view a crystalline electride as providing a *lattice gas* of nearly free electrons, confined to a tortuous set of cavities and channels, but with weak enough interelectron overlap to form a Mott insulator. In this paper I will focus on the geometric, experimental, and theoretical evidence for this picture of electrides.

Synthesis Methods and Problems

The synthesis of crystalline electrides is straightforward but difficult. One merely needs to dissolve stoichiometric amounts of the alkali metal and the complexant in a suitable solvent to form a solution of the complexed cation and the solvated electron and then grow crystals of the electride. For example, the "recipe" for the synthesis of $Cs^+(18\text{-crown-}6)_2e^-$ (in which Me_2O is dimethyl ether and Me_3N is trimethylamine) is as follows:

$$Cs(s) + 2[18C6(s)] \xrightarrow{Me_2O} Cs^+(18C6)_2 + e_{solv}^- \qquad (1)$$

Add Me_3N and slowly evaporate away the more volatile Me_2O to produce crystals. So much for the "straightforward" part!

The difficulties stem from the reactive nature of the alkali metal, the inherent thermodynamic instability of the complexant and solvent to reduction,[17] the need to avoid "contamination" with alkali metal anions, and the problems inherent in crystal growth. Over the years we have worked out a protocol to minimize decomposition, based on rigorous cleaning of the synthesis cell, vacuum-line synthesis methods, and the maintenance of temperatures below 230 K at all times during the synthesis. The reader is referred to a number of research and review articles for details of the synthesis methods, crystal growth, and structure determination.[5,14,15,18−33]

In spite of these precautions and a large number of attempts, we have been able to synthesize and determine the structures of only five electrides during the past 10 years. These are as follows: (1) $Cs^+(18\text{-crown-}6)_2e^-$ [abbreviated $Cs^+(18C6)_2e^-$]; (2) $Cs^+(15\text{-crown-}5)_2e^-$, [$Cs^+(15C5)_2e^-$]; (3) K^+(cryptand-[2.2.2])e^-, [$K^+(C222)e^-$]; (4) Li^+(cryptand[2.1.1])e^- [Li^+-$(C211)e^-$]; (5) mixed-sandwich electride [Cs^+(18-crown-6)(15-crown-5)$e^-]_6$·18-crown-6 [$Cs^+(18C6)(15C5)e^-$].

It is the correlation of the structures of these five electrides with optical, electronic, and magnetic properties that provides the "electron lattice gas" model referred to above. The synthesis of a crystalline electride does not guarantee that the mere avoidance of decomposition will lead to reproducible results. Three of the electrides, $Cs^+(18C6)_2e^-$, $Cs^+(15C5)_2e^-$, and $Li^+(C211)e^-$, exist in both crystalline and disordered forms, whose properties are very different.[20,23,33] To be certain of structure−property correlations, one needs to grow crystals and check their X-ray diffraction pattern and then maintain them below the temperature of an order−disorder transition. Early studies of these three electrides were complicated by the presence of such disordered phases, a phenomenon that was not suspected at the time.

Electrides have such high optical extinction coefficients that one can only study the absorption spectra of thin films (<3000 Å thick). Early optical studies were made with films produced by rapid solvent evaporation from a liquid film on an optical cell window.[34−36] This provided qualitative spectra but no control of thickness or uniformity. Quantitative spectra and four-probe conductivity of uniform films with known stoichi-

(16) Singh, D. J.; Krakauer, H.; Haas, C.; Pickett, W. E. *Nature* **1993**, *365*, 39−42.
(17) Cauliez, P. M.; Jackson, J. E.; Dye, J. L. *Tetrahedron Lett.* **1991**, *32*, 5039−5042.
(18) Dawes, S. B.; Ward, D. L.; Huang, R. H.; Dye, J. L. *J. Am. Chem. Soc.* **1986**, *108*, 3534−3535.
(19) Dawes, S. B.; Ward, D. L.; Fussa-Rydel, O.; Huang, R.-H.; Dye, J. L. *Inorg. Chem.* **1989**, *28*, 2132−2136.
(20) Dawes, S. B.; Eglin, J. L.; Moeggenborg, K. J.; Kim, J.; Dye, J. L. *J. Am. Chem. Soc.* **1991**, *113*, 1605−1609.
(21) Huang, R. H.; Faber, M. K.; Moeggenborg, K. J.; Ward, D. L.; Dye, J. L. *Nature* **1988**, *331*, 599−601.
(22) Wagner, M. J.; Huang, R. H.; Eglin, J. L.; Dye, J. L. *Nature* **1994**, *368*, 726−729.
(23) Wagner, M. J.; Huang, R. H.; Dye, J. L. *J. Phys. Chem.* **1993**, *97*, 3982−3984.
(24) Wagner, M. J.; Dye, J. L. *Annu. Rev. Mater. Sci.* **1993**, *23*, 223−253.
(25) Wagner, M. J.; Dye, J. L. *J. Solid State Chem.* **1995**, *117*, 309−317.
(26) Dye, J. L.; Ellaboudy, A. *Chem. Br.* **1984**, *20*, 210−215.
(27) Dye, J. L. *Prog. Inorg. Chem.* **1984**, *32*, 327−441.
(28) Dye, J. L. *Sci. Am.* **1987**, *257*, 66−75.
(29) Dye, J. L. In *Valency, The Robert A. Welch Foundation Conference on Chemical Research*; Robert A. Welch Foundation: Houston, TX, 1989; Vol. XXXII, pp 65−91.
(30) Dye, J. L. *Science* **1990**, *247*, 663−668.
(31) Dye, J. L.; Huang, R. H. *Chem. Br.* **1990**, *26*, 239−244.
(32) Dye, J. L. In *Physical Supramolecular Chemistry*; Echegoyen, L., Kiefer, A., Eds.; Kluwer Academic Publishers: Dordrecht, The Netherlands, 1996; pp 313−336.
(33) Huang, R. H.; Wagner, M. J.; Gilbert, D. J.; Reidy-Cedergren, K. A.; Ward, D. L.; Faber, M. K.; Dye, J. L. *J. Am. Chem. Soc.* **1997**, *119*, 3765−3772.
(34) DaGue, M. G.; Landers, J. S.; Lewis, H. L.; Dye, J. L. *Chem. Phys. Lett.* **1979**, *66*, 169−172.
(35) Dye, J. L.; Yemen, M. R.; DaGue, M. G.; Lehn, J.-M. *J. Chem. Phys.* **1978**, *68*, 1665−1670.
(36) Dye, J. L.; DaGue, M. G.; Yemen, M. R.; Landers, J. S.; Lewis, H. L. *J. Phys. Chem.* **1980**, *84*, 1096−1103.

ometry and thickness can now be obtained in favorable cases by high-vacuum codeposition of the alkali metal and the complexant.[37−41] Of course, this synthesis method provides no control over the crystallinity or crystallite orientation. One cannot, in fact, guarantee that a solid-state reaction will occur between the metal and complexant, although this usually appears to be the case.

Evidence for Electron Trapping in Cavities

Experimental Evidence. If the bulk of the "excess" electron density resides in the cavities, its average is only about 0.03 e^- $Å^{-3}$. Since the noise level in the X-ray diffraction studies typically gives peaks as high as 0.1 e^- $Å^{-3}$, we are unable to determine the location of the electron density from the crystal structure. Thus, experimental evidence for electron trapping in the anionic sites (cavities) must be indirect.

Probably the strongest experimental argument in favor of electron trapping *outside* of the complexed cation is the similarity of this complex to that found in alkalides and, indeed, in "normal" salts that contain the same complexed cation. The cation−oxygen and cation−nitrogen distances are essentially the same, and the geometry of the complexed ion is usually the same as well. This is illustrated in Figure 1, which shows the structures of the Li^+(C211) unit in the electride and the sodide.[33] Although the packing is different, the complexed cations are virtually identical in both compounds. In $Cs^+(18C6)_2e^-$ and $Cs^+(18C6)_2Na^-$ and the corresponding pair with the complexant (15C5), not only are the cation geometries the same, but also the crystal structures are very similar, the major difference being a slightly larger anionic site for Na^- than for e^-. If substantial electron density were present on the alkali cation or on the complexant, the cation binding would be weaker and we would expect a difference in distances and geometries.

Other indications of the "normalcy" of the complexed cation configuration are obtained from the ^{133}Cs NMR behavior.[42,43] The unpaired electron density at Cs^+ in polycrystalline samples of $Cs^+(18C6)_2e^-$, calculated from the temperature dependence of the chemical shift and the measured susceptibility, is only 0.056% of that for the cesium atom. For comparison, the percent atomic character of a 5 mol % metal cesium solution in ammonia is 3%, in methylamine is 5%, and in hexamethyl phosphoramide is 0.23% (see Table III in ref 43). Thus, the low value in the electride implies virtual exclusion of the unpaired electron density from the 6s orbital of the complexed Cs^+. In addition, the intercept at infinite temperature of the plot of the chemical shift vs $1/T$ is -67 ± 3 ppm, virtually identical with that in the corresponding sodide (−62 ppm), the iodide (−59 ppm), and the thiocyanate (−59 ppm).[42] The chemical shift of Cs is very sensitive to immediate surroundings, ranging from +232 ppm for the cesium cation in Cs^+(C222)-Cs^-(s) and +238 ppm in Cs^+(C222)SCN$^-$ to −238 ppm for the Cs^- anion in $Cs^+(18C6)_2Cs^-$.[43] The near constancy of the limiting chemical shift in the electride, sodide, and ordinary

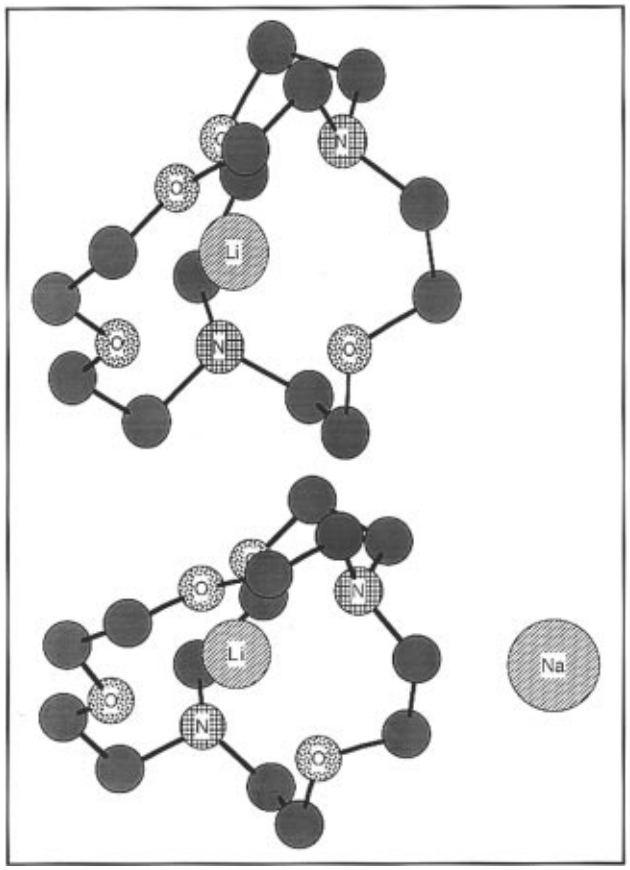

Figure 1. Comparison of the structures of the complexed cation in Li^+(C211)e^- and Li^+(C211)Na^-. The geometric arrangements of the atoms and the Li to O and Li to N distances in the electride and the sodide are virtually identical, supporting the assumption that the "excess" electron density in the electride does not penetrate substantially into the cryptand cage. Hydrogens have been omitted for clarity.

salts and the low percent atomic character argue strongly against substantial electron occupancy near the Cs^+ ion, as has been implied by Golden and Tuttle.[44,45]

In many cases, the EPR spectra of powdered electrides consist of nearly isotropic narrow lines at the free electron *g*-value. Exchange narrowing can cause collapse to a single line. Studies of $Cs^+(18C6)_2e^-$ and $Cs^+(18C6)_2Na^-$ at 9 and 250 GHz do show meaningful EPR results, however.[46] Although complicated by contamination with a disordered phase, the major spectral component is very similar in these two materials. Defect electrons in the sodide almost certainly occupy the anionic sites, implying that the unpaired electrons in the electride are also trapped at these sites.

The most detailed and convincing evidence that defect electrons in sodides are trapped at empty Na^- sites comes from EPR, ENDOR, and ESEEM studies of defect electrons in the sodide Cs^+(HMHCY)Na^-, in which HMHCY is hexamethyl hexacyclen.[47,48] The crystal structure of this sodide shows that Cs^+ is contained in a cup-shaped cavity formed by HMHCY and that it is in contact with Na^-.[49] Defect electrons in the

(37) Le, L. D.; Issa, D.; VanEck, B.; Dye, J. L. *J. Phys. Chem.* **1982**, *86*, 7−10.
(38) Jaenicke, S.; Faber, M. K.; Dye, J. L.; Pratt, W. P., Jr. *J. Solid State Chem.* **1987**, *68*, 239−246.
(39) Skowyra, J. B.; Dye, J. L.; Pratt, W. P., Jr. *Rev. Sci. Instrum.* **1989**, *60*, 2666−2672.
(40) Hendrickson, J. E.; Kuo, C. T.; Xie, Q.; Pratt, W. P., Jr.; Dye, J. L. *J. Phys. Chem.* **1996**, *100*, 3395−3401.
(41) Hendrickson, J. E.; Xu, G.; Pratt, W. P., Jr.; Dye, J. L. *J. Phys. Chem. A* **1997**, *101*, 4149−4155.
(42) Dawes, S. B. Ph.D. Dissertation, Michigan State University, East Lansing, MI, 1986.
(43) Dawes, S. B.; Ellaboudy, A. S.; Dye, J. L. *J. Am. Chem. Soc.* **1987**, *109*, 3508−3513.
(44) Golden, S.; Tuttle, T. R., Jr. *Phys. Rev. B.* **1992**, *45*, 913−918.
(45) Golden, S.; Tuttle, T. R., Jr. *Phys. Rev. B.* **1994**, *50*, 8059−8062.
(46) Shin, D. H.; Dye, J. L.; Budil, D. E.; Earle, K. A.; Freed, J. H. *J. Phys. Chem.* **1993**, *97*, 1213−1219.
(47) Ellaboudy, A. S.; Bender, C. J.; Kim, J.; Shin, D.; Kuchenmeister, M. E.; Babcock, G. T.; Dye, J. L. *J. Am. Chem. Soc.* **1991**, *113*, 2347−2352.
(48) McCracken, J.; Shin, D.; Dye, J. L. *Appl. Magn. Reson.* **1992**, *3*, 305−316.
(49) Kuchenmeister, M. E.; Dye, J. L. *J. Am. Chem. Soc.* **1989**, *111*, 935−938.

sodide show strong hyperfine coupling to one Cs^+ ion,[47] in agreement with electron trapping at this site. ENDOR (electron−nuclear double resonance) spectra show coupling to the CH_3−N protons and to "distant" Na^- and Cs^+ ions.[47] Finally, ESEEM (electron spin echo envelope modulation) spectra show coupling to the Cs^+ ion "across" the cavity from the exposed Cs^+ as well as to the four other nearest Cs^+ ions.[48] These interactions clearly imply defect electron occupancy at the empty Na^- site. We conclude that empty anionic sites, whether in an alkalide or an electride, are natural trapping sites for electrons.

The role of electron−electron coupling will be considered in detail later. Here we merely draw attention to the strong coupling in $K^+(C222)e^-$ that implies formation of electron "dimers". The unusual structure of the potasside, $K^+(C222)K^-$, is very similar to that of the electride and contains $(K^-)_2$ dimers in very open dumbbell-shaped cavities.[50] Thus, electron occupancy of the closely-spaced anionic sites in this electride would be expected to yield strong pairwise electron coupling. It should be noted that the complexed cation $K^+(C222)$ has the same structure and the same powder ^{39}K NMR pattern in $K^+(C222)e^-$ and in $K^+(C222)K^-$.[51] Once again, all of these results provide experimental evidence for electron trapping in cavities.

Theoretical Evidence. There have been three quantum-mechanical studies of electrides. The first of these was a self-consistent tight-binding Hartree−Fock calculation for $Cs^+(18C6)_2e^-$.[52] The calculations indicated that occupancy of the empty 6s orbital of Cs^+ would yield an energy above the conduction band. Construction of a "cavity-centered" hydrogen-like orbital that utilized the image positive charge at the cavity yielded a stable structure. Although this treatment was only semi-empirical, it provided a rationale for electron trapping in the cavity.

The second theoretical approach focused on the single molecule properties of the hypothetical molecules Li(9C3) and $Li(9C3)_2$.[53−55] Various levels of *ab-initio* calculations were performed, concluding with unrestricted Hartree−Fock calculations at the 6-31G++** level. The Li *2s* electron in the former molecule is moved by the complexant into a hybrid sp^3-like empty orbital. In the sandwich complex the excess electron becomes "squeezed" out as the distance between the lithium and the 9C3 molecules decreases to the equilibrium value. The final state of the excess electron is Rydberg-like, with a decrease of about 3 orders of magnitude in the atomic character of Li. The authors concluded that the isolated $Li(9C3)_2$ molecule behaves as an "expanded atom". It does not require much imagination to conclude that electron-trapping would occur outside of the complexed cation if the $Li(9C3)_2$ molecules were brought together to form a crystal.

The same authors who carried out the calculations on the $Li(9C3)_2$ molecule also constructed a simple model of $Cs^+(18C6)_2e^-$ to explain the origin of the electron exclusion from the vicinity of the cation.[53,54] This model considered the molecule as two uniformly charged spherical shells around a central Cs^+ ion, a charge distribution that corresponds to the negative oxygens and positive hydrogens of the crown ethers. It was shown by solving the radial Schrödinger equation that the 6s electron of Cs moved further and further out as the charges on the shells increased. When each of the crown ether oxygens carried a fractional charge of 0.8 e, the unpaired electron density moved outside of the complexant and the calculated percent atomic character of cesium in $Cs^+(15C5)_2e^-$ also agreed with the experimental value.

The most sophisticated quantum calculations for a crystalline electride are those of Singh et al.[16] These authors used our crystal structure of $Cs^+(15C5)_2e^-$ to carry out local density functional approximation (LDA) calculations with an *ab-initio* mixed basis method. These calculations clearly showed that the excess electrons are localized in the cavities because of the reduction in their kinetic energy. They also showed that electron density tended to be excluded from the complexed cations and to extend into the void spaces and channels that interconnect the cavities.

In summary, the experimental and theoretical evidence for electron trapping at the anionic sites in electrides is very strong. This does not exclude "leakage" of the electron density into surrounding regions of the crystal, but it does imply that orthogonality of the wave function to those of the closed-shell electrons of the complexant (the Pauli exclusion principle in action) tends to move most of the electron density into the void spaces.

Evidence for Electron−Electron Coupling through Channels

Having concluded that excess electron density tends to pile-up in the cavities in electrides, we turn our attention to the nature of interelectron coupling. The magnitude of such coupling is indicated by the value of the coupling constant, J, conveniently expressed in degrees Kelvin by reporting $-J/k_B$, in which k_B is the Boltzmann constant and the negative sign reflects the antiferromagnetic nature of the coupling in electrides. (We use the convention for J common in magnetochemistry.[56]) When the molar magnetic susceptibility of a polycrystalline sample, χ_m, has a maximum at some temperature T_m, the value of $-J/k_B$ is roughly equal to this temperature. To obtain a more accurate value requires that the data be fit by a theoretical expression. The correct expression to use is not obvious and requires information about the geometry and the likely coupling mechanism. Because the EPR spectra of electrides show nearly isotropic *g*-values, the Heisenberg spin Hamiltonian

$$H = -2\sum_{i \neq j} J_{ij} \hat{\mathbf{S}}_i \cdot \hat{\mathbf{S}}_j \qquad (2)$$

is appropriate. The sum is over all interacting spins in the system, and J is negative for antiferromagnetic interactions.

The magnitude of J depends on the extent of overlap of the wave functions of spins i and j. Since we consider the excess electron population to reside primarily in voids in the structure, it is natural to ask whether we can correlate the dimensionality of the coupling and the magnitude of J with the geometry and "openness" of the channels that connect the cavities. It quickly becomes obvious that there is little or no correlation with just the intercavity distance. The cavities in $Cs^+(15C5)_2e^-$ are closer together than those in $Cs^+(18C6)_2e^-$, yet the latter has a $-J$ value that is 10 times as large. Even more striking is the dramatic drop in $-J/k_B$ from ∼50 to ∼2 K for $Cs^+(18C6)_2e^-$

(50) Huang, R. H.; Ward, D. L.; Dye, J. L. *J. Am. Chem. Soc.* **1989**, *111*, 5707−5708.
(51) Kim, J.; Eglin, J. L.; Ellaboudy, A. S.; McMills, L. E. H.; Huang, S.; Dye, J. L. *J. Phys. Chem.* **1996**, *100*, 2885−2891.
(52) Allan, G.; DeBacker, M. G.; Lannoo, M.; Lefebvre, J. *Europhys. Lett.* **1990**, *11*, 49−53.
(53) Rencsok, R.; Kaplan, T. A.; Harrison, J. F. *J. Chem. Phys.* **1990**, *93*, 5875−5882.
(54) Rencsok, R.; Kaplan, T. A.; Harrison, J. F. *J. Chem. Phys.* **1993**, *98*, 9758−9764.
(55) Kaplan, T. A.; Rencsok, R.; Harrison, J. F. *Phys. Rev. B.* **1994**, *50*, 8054−8058.
(56) Carlin, R. L. In *Magnetocemistry*; Springer-Verlag: Berlin, 1986; p 71.

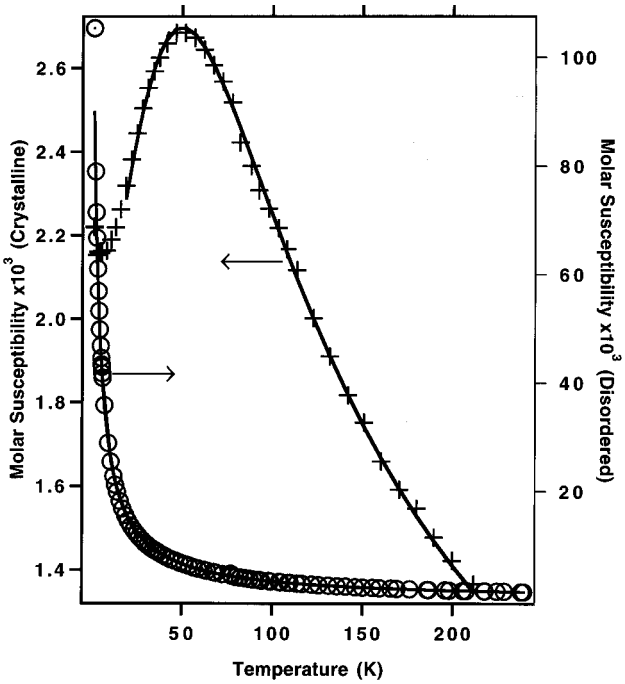

Figure 2. Temperature dependence of the molar magnetic susceptibilities of crushed single crystals of $Cs^+(18C6)_2e^-$ (top curve) and of the same sample after heating above the order−disorder temperature of ∼230 K (bottom curve). Disordered samples follow the Curie−Weiss equation (solid line) with a Weiss constant of only ∼−2 K. Clearly, disorder has virtually eliminated interelectron coupling in the crystalline sample, evidenced by the agreement of the susceptibility to the linear chain Heisenberg antiferromagnetic model (solid line).

following the order−disorder transition.[23] We have lost very few electrons to decomposition, but the coupling virtually disappears! The same phenomenon occurs for $Cs^+(15C5)_2e^-$, but it is less dramatic since $-J/k_B$ is only ∼4 K for the crystalline phase. The striking effect of disorder on the magnetic susceptibility is shown for $Cs^+(18C6)_2e^-$ in Figure 2. Clearly something other than interelectron distance is involved. As we shall see later, the dimensionalities, diameters, and lengths of the "empty" channels that connect the cavities play major roles and permit rationalization of the observed magnetic susceptibilities.

Visualization of Cavities and Channels

The usual display of crystal structures shows the structure of a molecule or a collection of atoms, ions, or molecules. For example, Figure 3a shows the molecular packing in the electride $Li^+(C211)e^-$.[33] The structure of one molecule was shown in Figure 1. Because of the ball-and-stick nature of the display shown in Figure 3a, the atomic sizes are not well represented. On the other hand, a space-filling representation such as that shown in Figure 3b is so cluttered that it is difficult to visualize the geometry of the void spaces.

As indicated previously, the features that are most important in understanding the optical, magnetic, and electronic properties of electrides are the sizes and shapes of the cavities and of the interconnecting channels. The cavity−channel geometry is very difficult to determine just by inspection of the molecular packing. To help understand the locations of molecules and void spaces in electrides, Figure 4 shows a ball-and-stick model of $Cs^+(15C5)_2e^-$ with the major features labeled. In order to provide more useful images and to determine the sizes of cavities and the minimum diameters of the interconnecting channels,

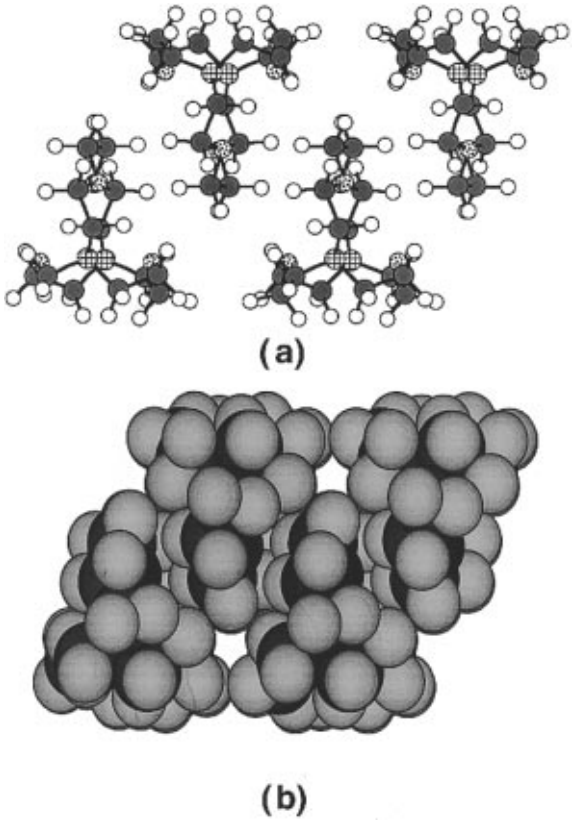

Figure 3. Molecular packing in the electride $Li^+(C211)e^-$: (a) Ball-and-stick model with atom sizes not to scale; (b) space-filling model of four $Li^+(C211)$ units. The geometries of the cavities and channels are difficult to visualize with this type of representation even though void spaces in electrides can account for up to half the total volume.

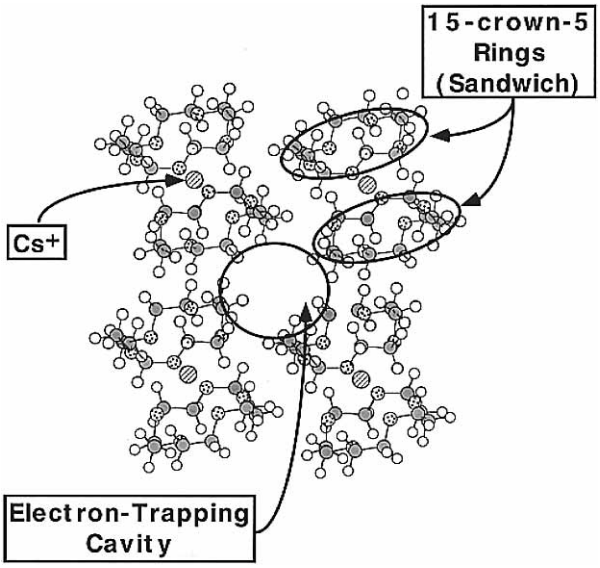

Figure 4. Ball-and-stick model of the crown-ether sandwich electride $Cs^+(15C5)_2e^-$ with identification of the major features of interest.

we have developed programs[57] that can couple commercial structural computer packages, such as BIOGRAF[58] or BIOSYM,[59] to 3D visualization packages, such as AVS[60] or EXPLORER,[61] to produce 3D images of the cavities and

(57) The programs and a description of their use are available by anonymous FTP to *argus.cem.msu.edu* with the path *pub/dye/voids*.
(58) Molecular Simulations Inc., 16 New England Executive Park, Burlington, MA 01803-5297.
(59) Biosym Technologies, 9685 Scranton Road, San Diego, CA 92121-2777.
(60) Advanced Visual Systems, Inc., 300 Fifth Ave., Waltham, MA 02154.

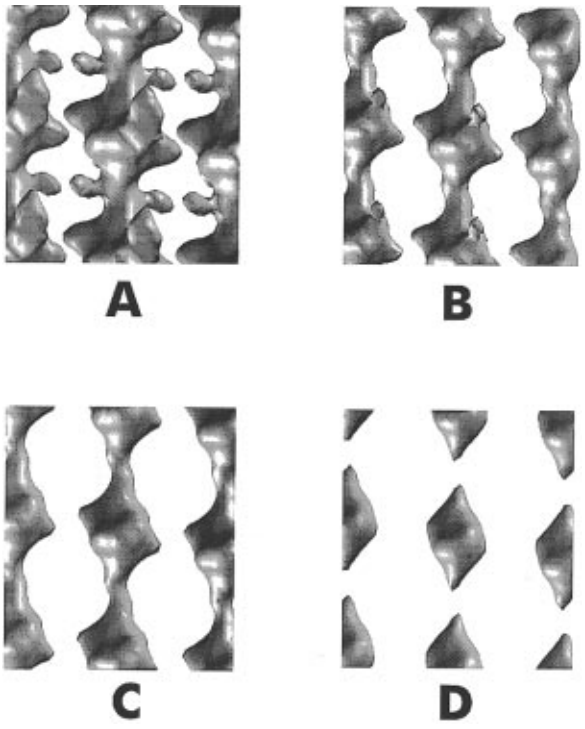

Figure 5. Cavity−channel "geometries" of $Cs^+(15C5)_2e^-$ at four distances from the van der Waals surfaces of the molecules. A small sphere of radius 0.31 Å (view A) could "roll" into side "pockets" but would be too large to move from one chain to another. Views B−D are at 0.43, 0.54, and 0.86 Å, respectively. By noting that the major vertical channel just disappears at a distance of 0.75 Å, we can determine that a hard sphere of this radius would just fit through the channel from one cavity to another. The cavities disappear at a setting of 2.07 Å, corresponding to a close fit of a sphere of 4.14 Å diameter.

channels. These images can be rotated on screen or printed from any perspective to provide views of the geometry of the void spaces. In addition, one can easily determine the size of the largest sphere that can fit into a cavity or pass through a channel. The effective dimensionality of the cavity−channel system can be easily seen, and the lengths and diameters of the channels can be determined.

The program uses "hard sphere" van der Waals radii of the atoms, together with the crystal structure and enough unit cells to form a cube about 30 Å on an edge, to create a cubic grid of points within the void spaces. Usually, the cube is provided with a $40 \times 40 \times 40$ or $80 \times 80 \times 80$ point grid. Each point is assigned a number from 0 to 255 that is proportional to the distance from the grid point to the nearest atomic van der Waals surface. The radius of the largest sphere that can fit into a cavity corresponds to the value 255. The largest value found in a channel then corresponds to the radius of the largest hard sphere that could just pass through the channel. Connecting all points that have unit value with an isosurface display routine would give the shape of the total void space, subject to the resolution of the grid. Such an isosurface is not very useful, however, because the outer regions obscure the cavity−channel geometry inside the display and it is very cluttered. To visualize the cavity−channel geometry more favorably, the data are smoothed to avoid abrupt changes in slope, and isosurfaces at selected distances from the atomic surfaces are chosen in order to avoid obstruction of the view and to eliminate minor void spaces such as the myriad "crevices" that exist between packed spheres. The results do not display the true shapes of the void spaces but rather the locus of all points that could be covered by the center of a contacting sphere of radius equal to the distance from the van der Waals surfaces. Similar representations are used by commercial programs such as BIOSYM[59] to locate "solvent-accessible sites".

Figure 5 illustrates the cavity−channel views that result from different choices of the distance parameter. It shows the cavity−channel isosurfaces of $Cs^+(15C5)_2e^-$ at various distances from the van der Waals surfaces of the complexed cation. View A at 0.31 Å gives the most accurate picture of the shapes of the void spaces. Even though this view is complicated by projection of the void spaces into the centers of the crown ether molecules (right and left projections), it is clear that the cavities are interconnected by a major vertical channel. Interchain connections must have diameters smaller than 0.62 Å since a sphere of radius 0.31 Å cannot pass from one chain to the next. Indeed, by decreasing the distance to the van der Waals surfaces to 0.28 Å, we find that interchain channels just form, corresponding to a channel diameter of 0.56 Å at the narrowest point. The image of the major vertical channel just disappears between views C and D of Figure 5 and corresponds to a minimum diameter of 1.5 Å. By measuring the distance to the van der Waals surfaces at which the cavity just disappears, we find that a sphere of diameter 4.14 Å would just "touch" the hydrogens of the complexant. Of course, atoms are not hard spheres, the electron density does not go abruptly to zero at the van der Waals radius of an atom, and the positive charge on the H atoms caused by the O−C−H dipoles would be attractive to electron density. Thus, the diameter of 4.14 Å for the electron density sphere in the cavity does not preclude substantial overlap with the hydrogens that line the cavity.

It was noted earlier that the electron density distribution in $Cs^+(15C5)_2e^-$ was calculated by the LDA method. As shown in Figure 2 of ref 6, the isosurfaces that correspond to various calculated electron density values are remarkably similar to the void space isosurfaces obtained from the crystal structure. The only major difference was a bulge in the calculated electron density near the hydrogens, again indicating the attraction of the positive hydrogen for the trapped electron.

The similarity between the calculated electron density isosurfaces and the geometric void isosurfaces is so striking that we are tempted to use the latter as first approximations to the electron density distributions in other electrides. This permits a qualitative assessment of the degree of overlap of electron density in adjacent cavities. These considerations, in turn, allow us to understand the effective dimensionalities of the electron−electron coupling and the relative sizes of the coupling constants, $-J/k_B$.

Magnetic Behavior of Electrides

Magnetic Susceptibilities. Three crystalline electrides, $Cs^+(15C5)_2e^-$, $Cs^+(18C6)_2e^-$, and $Li^+(C211)e^-$, have essentially 1D cavity−channel geometries with interchain channels that are either long, of small diameter, or both. The reader is referred to Figures 1, 3, and 5 of ref 6 for views of the cavity−channel geometries of these three electrides. Cavity diameters, major channel minimum diameters and cross-sectional areas, and the diameters of secondary channels are given in Table 1. Also given are the coupling constants ($-J/k_B$) and A obtained from eq 5 (see below). All three electrides also form apparently disordered phases with smaller coupling constants than those of the crystalline phase (see Figure 2). Although the structures of the disordered phases are not known, the most likely reason for the decrease in $-J/k_B$ is blockage of the major channels by

(61) Iris Explorer Center, 1400 Opus Place, Suite 200, Downers Grove, IL 60515−5702.

Table 1. Cavity and Channel Diameters, Minimum Channel Cross-Sectional Areas, and Magnetic Coupling Constants for Four Electrides

	cavity diam (Å)	major channel		params from eq 5		secondary channel diam (Å)
		diam (Å)	area (Å^2)	$-J/k_B$ (K)	A	
$Cs^+(15C5)_2e^-$	4.1	1.49	2.3	3.0	1.17, 0.69	0.56
$Cs^+(18C6)_2e^-$	4.8	1.95[a]	10.9	38	0.94	1.5
$Li^+(C211)e^-$	4.4	2.4	12.5	54	1.04	1.5
$K^+(C222)e^-$	4.6	4.0	21.0	~430[b]	1.0[b]	3.3, 2.2

[a] The major channel in $Cs^+(18C6)_2e^-$ has a "dumbbell"-shaped cross section through which two spheres of diameter 1.95 Å could pass simultaneously. [b] Fit is to alternating chain Heisenberg model with $-J/k_B = 430$ K, $-J'/k_B = 370$ K, with the equivalent of A fixed at 1.0. Only a short region well below the presumed maximum can be measured, so the coupling constants are not well determined.

complexant reorganization. The structure−property correlations described below apply only to the phases of known structure.

The magnetic susceptibilities of these three electrides are shown as functions of temperature in Figure 6. Both $Cs^+(18C6)_2e^-$ and $Li^+(C211)e^-$ show broad maxima in the susceptibility rather than the sharp cusp expected for a 3D antiferromagnet with a first-order Néel transition. The situation is not so clear with $Cs^+(15C5)_2e^-$, whose susceptibility maximum occurs at 4.6 K, but even in this case the data exhibit a smooth maximum rather than an abrupt transition. This first indication of lower dimensionality agrees with the cavity−channel picture of essentially 1D chains of trapped electrons that interact with their neighbors through connecting channels.

The second indication of the importance of channels is the dramatic shift of the susceptibility maximum from 4.6 to 50 to 70 K for crystalline $Cs^+(15C5)_2e^-$, $Cs^+(18C6)_2e^-$, and $Li^+(C211)e^-$, respectively. This trend agrees with the increased size of the connecting channels (see Table 1) in this series of electrides.

Finally, the susceptibilities of these three electrides are in accord with theoretical predictions for linear chain Heisenberg antiferromagnetic (LCHA) behavior. For an infinite chain of identical spins with only first neighbor interactions, the Heisenberg Hamiltonian (eq 2) becomes

$$H = -2\sum_i \hat{S}_i \cdot \hat{S}_{i+1} \tag{3}$$

Finite chain calculations were extrapolated to infinite chain length by Bonner and Fisher.[62] For $J < 0$ (antiferromagnetic), these extrapolations can be accurately represented by the expression for the molar susceptibility[63]

$$\chi_m = \frac{Ng^2\mu_B^2}{k_B T}\left[\frac{0.25 + 0.14995y + 0.30094y^2}{1 + 1.9862y + 0.68854y^2 + 6.0626y^3}\right] \tag{4}$$

in which $y = |J|/kT$. The values of $-J/k_B$ and A given in Table 1 were obtained by least-squares fits of the measured molar magnetic susceptibility, χ_m, by the equation

$$\chi_m(T) = A\chi_m(y) + B \tag{5}$$

with adjustment of A, B and J. Equation 4 is not valid at temperatures far below that of the maximum, where other complications such as a "Curie tail", a spin-Peierls transition [for $Li^+(C211)e^-$],[33] and the onset of interchain coupling cause it to be invalid. For these reasons the temperature range of the least-squares fitting procedure was restricted to 20 K and above for $Li^+(C211)e^-$ and $Cs^+(18C6)_2e^-$ and to 3 K and above for $Cs^+(15C5)_2e^-$.

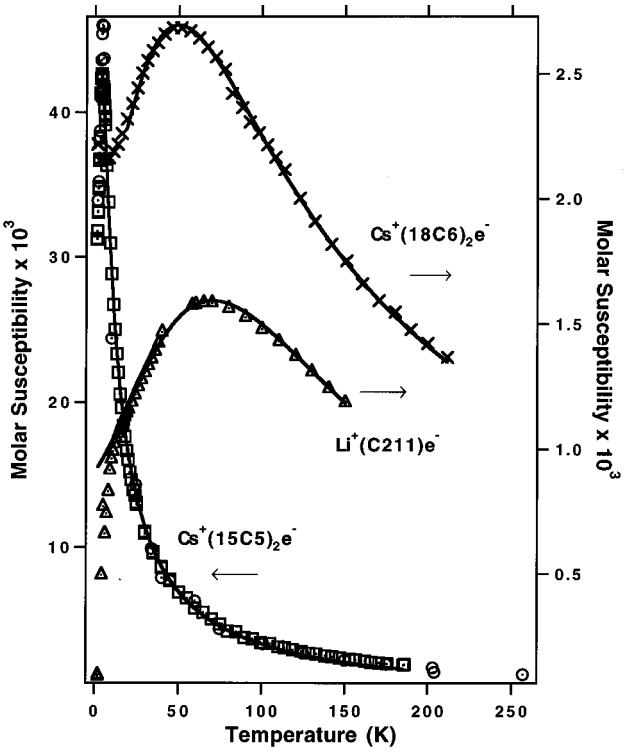

Figure 6. Temperature dependence of the molar magnetic susceptibilities of three electrides that have essentially 1D cavity−channel geometries. In each case, the solid line represents the least-squares fit by the LCHA model (eq 5). Note that the left scale refers to $Cs^+(15C5)_2e^-$, while the right scale is for $Cs^+(18C6)_2e^-$ and $Li^+(C211)e^-$. The data for one of the two runs with $Cs^+(15C5)_2e^-$ (represented by squares) were divided by 0.60 to compensate for an apparent incorrect sample mass (see text). Data represented by circles, and all data for the other two electrides, were as measured except for subtraction of a low temperature "Curie tail".

For a pure electride A should be 1.0, but weighing errors, partial decomposition, the presence of complexant that could not be completely removed by rinsing, and the presence of some noncrystalline phase can cause deviations from unity. The value of B depends upon whether the magnetization of a decomposed sample plus the container or just that of the container is subtracted from the measured total magnetization.

The calculated molar susceptibilities according to eqs 4 and 5 are shown as solid lines in Figure 6. The peak in the susceptibility of $Cs^+(15C5)_2e^-$ occurs at such a low temperature that other interactions could interfere and the LCHA model can only be said to be compatible with the data but not unique. On the other hand, the fits to the data for $Cs^+(18C6)_2e^-$ and $Li^+(C211)e^-$ are remarkably good and yield strong support for the 1D chain model. Other models such as various mean-field treatments, spin dimerization, and 3D antiferromagnetism, etc., do not fit the data at all well. Of particular importance is the magnitude of the susceptibility at the peak. In all cases, except for the two runs with $Cs^+(15C5)_2e^-$, nearly 100% of the spins are accounted for. The peak susceptibility in the LCHA model is particularly sensitive to the value of the coupling constant, $-J$. Note that the molar susceptibility at the maximum varies from 46×10^{-3} to 2.7×10^{-3} to 1.6×10^{-3} mol^{-1} for $Cs^+(15C5)_2e^-$, $Cs^+(18C6)_2e^-$, and $Li^+(C211)e^-$, respectively. Yet in all three cases, the LCHA model fits the data and the A values are within 6% of unity for the latter two electrides.

(62) Bonner, J. C.; Fisher, M. E. *Phys. Rev. A* **1964**, *135*, 640−658.

(63) Estes, W. E.; Gavel, D. P.; Hatfield, W. E.; Hodgson, D. *Inorg. Chem.* **1978**, *17*, 1415−1421.

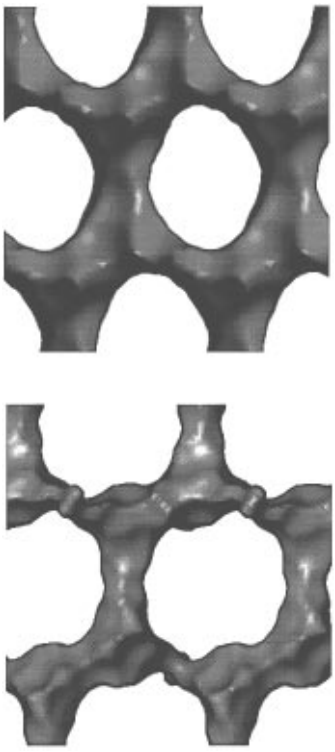

Figure 7. Comparison of the single plane cavity−channel geometry of $K^+(C222)e^-$ (bottom figure) with that of $K^+(C222)K^-$ (top figure). To construct the latter figure, the K^- ions were removed from the array of molecules so that the cavities in this figure represent "emptied" K^- sites. Note the geometric similarities between the potasside and the electride. A major difference (not shown here) is that the cavity−channel geometry in the electride is essentially 2D in nature while the potasside has equal-size channels connecting each "chain" with four neighboring chains to create a 3D cavity−channel structure.

Only $Li^+(C211)e^-$ among the electrides shows a spin-Peierls transition.[33] Such transitions typically involve lattice distortions because of electron−phonon coupling. In this electride, however, it is possible that the transition is driven by the "spin-frustration" that is a consequence of the spin-ladder-like geometry of the cavity−channel chains.[33] As seen in Figure 5 of ref 6, the cavities in the electride are connected not only to the nearest-neighbor cavities by channels of diameter 2.4 Å, but also to next-nearest neighbors, albeit through narrower channels of diameter 1.5 Å. In such a system, a spin-Peierls transition would only require electron pairing along the major channels by relatively minor shifts of the electron density, which would relieve to some extent the competition from next-nearest neighbors. This could occur with minimum lattice distortion.[33] However, it should be noted that the LCHA model with only a single value of $-J$ fits the data down to the spin-Peierls transition temperature.

$K^+(C222)e^-$ Susceptibility. What a surprise it was to find that K^- and Rb^- in $K^+(C222)K^-$ and $Rb^+(C222)Rb^-$ formed *dimers* of the anions! The anion-anion distances were not the usual 7−8 Å but rather only 4.90 Å in the potasside and 5.13 Å in the rubidide, each about 1 Å shorter than the sum of the van der Waals radii of two anions. Subsequent theoretical calculations on $(K^-)_2$ dimers in the vicinity of positive charges indicated that partial sp hybridization can stabilize bonding between such unlikely partners.[64] It also provides rationalization of close-contact chain formation[50] in $Cs^+(C222)Cs^-$ and $Rb^+(18C6)Rb^-$, in which hybridization would permit formation of two weak bonds for each anion. While such dimers and chains would not be stable in the gas phase, the proximity of complexed alkali metal cations could minimize the effects of Coulomb repulsion between adjacent anions.[64]

The electride $K^+(C222)e^-$ has a cavity−channel geometry that is very similar to that of $K^+(C222)K^-$ with the K^- anion removed. A comparison is shown in Figure 7. The rubidide is isostructural to the potasside with only slightly larger cavities to accommodate Rb^-. The similarity in the trapping sites for K^- or Rb^- and e^- suggest the presence of strong pairwise electron coupling in the electride.

In this electride each cavity has a diameter of 4.6 Å and the channel diameters between electrons in the pair is 4.0 Å, while that between pairs is 3.3 Å. Along the major chain direction then, all channels are rather open and we visualize an electron density distribution that is spread out more than in other electrides. The chains are interconnected by U-shaped channels of minimum diameter 2.2 Å to form a 2D "lattice" of cavities and channels (see Figure 4 of ref 6).

The magnetic susceptibility of this electride as a function of temperature (after subtracting a "Curie tail") shows a spin-paired ground state and strong coupling. Even at 200 K, the susceptibility is only 15% of that for fully unpaired electrons and it is still increasing. Originally, the interpretation we gave to these results was based on a singlet dimer with either dissociation or formation of a triplet state. Additional measurements of the magnetic susceptibility over a wider temperature range and with cycling of the temperature are more compatible with an alternating linear chain Heisenberg antiferromagnetic (ALCHA) model.[65] The appropriate spin Hamiltonian is

$$H = -2J\sum_{i=1}^{n/2}[\hat{\boldsymbol{S}}_{2i}\cdot\hat{\boldsymbol{S}}_{2i-1} + \alpha\hat{\boldsymbol{S}}_{2i}\cdot\hat{\boldsymbol{S}}_{2i+1}] \qquad (6)$$

in which J represents the pairwise coupling of the electron "dimer" in the dumbbell-shaped cavity and α represents the coupling of the electron with its other nearest neighbor.

After subtraction of a "Curie tail" from the magnetic susceptibility data, a fit by the ALCHA model with an appropriate fitting function based on numerical calculations is good and yields $-J/k_B = 430$ K and $\alpha = 0.83$. Because of thermal decomposition of the electride, an upper limit on T is 250 K. While these limited data cannot confirm the validity of ALCHA model, they are not compatible with a simple dimer model, with a singlet−triplet equilibrium, or with the simpler LCHA model. Once again, the interaction model used to fit the data can be related to the cavity−channel structure. In particular, the large values of both coupling constants is what would be expected because of the very open channels in this electride.

A Mixed-Sandwich Electride. The most complex electride was synthesized from cesium metal and a mixture of 18C6 and 15C5. Its structure, cavity−channel geometry, and properties have been described in detail elsewhere.[22,25] The complexity of the void geometry, as well as the beauty that can be created by computer-rendering in color of an actual structure, is indicated in Figure 8. The formula $[Cs^+(18C6)(15C5)e^-]_6\cdot 18C6$ is indicative of the complexity. Each cesium cation is complexed by a 15C5 molecule and an 18C6 molecule. These sandwich complexes form a six-membered ring around a central "free" 18C6 molecule. Spin-pairing is strong, with only about 9% of the susceptibility expected for independent spins at 170 K. The structure is much too complex and the temperature

(64) Tientega, F.; Dye, J. L.; Harrison, J. F. *J. Am. Chem. Soc.* **1991**, *113*, 3206−3208.

(65) Wagner, M. J. Ph.D. Dissertation, Michigan State University, East Lansing, MI, 1994.

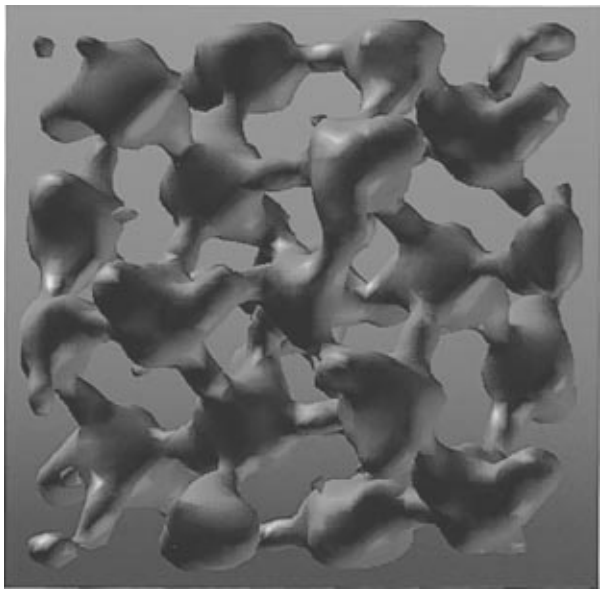

Figure 8. Color view of the cavity−channel structure of the mixed-sandwich electride, $[Cs^+(15C5)(18C6)e^-]_6 \cdot 18C6$. This view is down the 3-fold symmetry axis with an "extra" 18C6 molecule in the center, below the small triangular-shaped vacancy. For details, see ref 25. I am indebted to Peter Carrington for color enhancement.

range is too small to permit us to pin down the nature of the spin-pairing interactions. The data are, however, compatible with the spin Hamiltonian of a six-membered ring, yielding $-J/k_B \sim 400$ K.[25] In addition there is a substantial "Curie tail" that corresponds to as much as 4−5% defect electrons and whose magnitude depends on the preparation.

The susceptibility behavior of a single electride cannot tell us much about the nature of the electron−electron interactions. But the good correspondence between the dimensionality and size of the connecting channels and the magnetic behavior lends strong support to the importance of the geometry of the void spaces. Figure 9 shows the correlation between the cross-sectional area of the channels and the coupling constant, $-J$ [displayed as $\ln(-J/k_B)$]. Thus, the magnetic susceptibility provides strong justification for the view that electrides contain a "confined electron lattice gas".

Optical Spectra and Conductivity

The existence of solid electrides was hinted at as early as 1974 when we prepared "blue, strongly paramagnetic solids" by evaporation of solvent from solutions that contained M^+-(C222) and e_{solv}^-. The first strong evidence for electrides was obtained in 1978 from the absorption spectrum of solvent-free thin films obtained by flash-evaporation of solutions of K^+-(C222), e_{solv}^- in $MeNH_2$ on an optical cell window.[35] The IR peak obtained resembled that of solvated electrons, although no solvent remained. We first used the term "electride" in the publication that reported these results.[35]

The optical spectra of solvent-evaporated alkalide and electride thin films proved to be an easy way to identify the species present. The peaks shift uniformly to lower energies as one proceeds in the following order: Na^-, K^-, Rb^-, Cs^-, e^-. The problems with solvent-evaporated thin films were lack of uniformity and the absence of control over thickness. These difficulties were removed by controlled coevaporation of the alkali metal and the complexant under high vacuum in a bell-jar.[38−40] Excellent quantitative spectra were obtained with $Na^+(C222)Na^-$, formed by a rapid solid-state reaction of codeposited sodium with C222.[40]

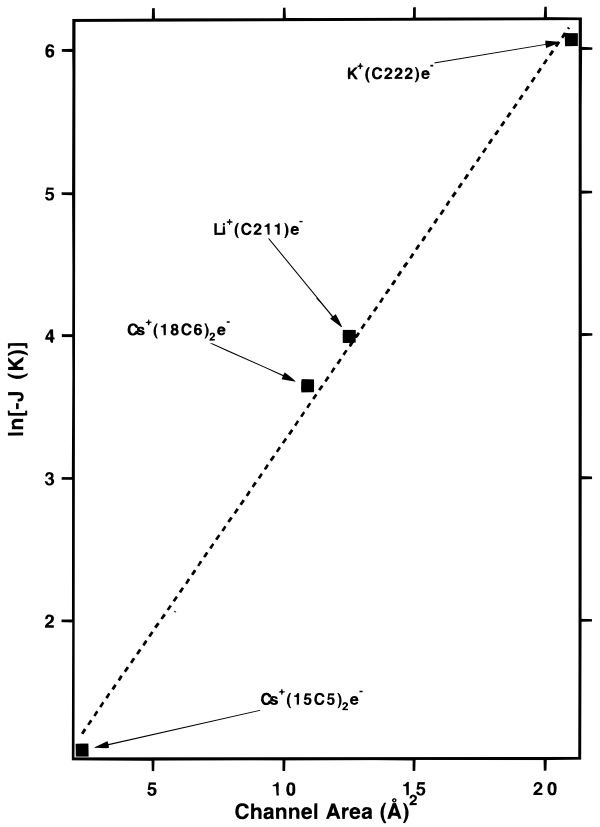

Figure 9. Correlation between the coupling constants [plotted as $\ln(-J/k_B)$] and the minimum cross-sectional areas of the major channels in four electrides. Each area was determined (at the narrowest position in the channel) by extrapolating the area as a function of the distance from the molecular van der Waals surfaces to zero distance.

We noted in early experiments that rapid evaporation of $MeNH_2$ from potassium−C222 solutions at dry-ice temperatures initially yielded a K^- peak that evolved into a plasmalike absorption spectrum. Such a spectrum also forms from $K-NH_3$ solutions that contain C222 and is virtually indistinguishable from that of a metallic solution of K in NH_3.[34] Also, the powder conductivity[66] of $K^+(C222)e^-$ was as high as 20 Ω^{-1} cm^{-1} a value as much as 10^{10} times higher than that of other electrides. The conductivity−temperature behavior of the five electrides of known structure is shown in Figure 10. Because of the near-metallic behavior of $K^+(C222)e^-$, we initiated an extensive series of optical and conductivity studies of codeposited thin films of K and C222. The results are complex and interesting and will be described in detail in a separate publication. When the ratio of K to C222 is 2:1, an insulating film of $K^+(C222)K^-$ is formed with the typical K^- absorption peak at 850 nm (1.46 eV) plus an electride peak at 1400 nm (0.89 eV). When the ratio is 1:1 (at $T < 200$ K), an initial peak of K^- decays to the plasmalike absorption spectrum of the electride. Both 2-probe and 4-probe conductivity studies of ∼2000 Å thick films yield specific conductances (as high as 30 Ω^{-1} cm^{-1}) and activation energies (∼30 meV) comparable to those obtained with powders. One of the most puzzling features in this work was the behavior of the conductivity during film decomposition. As with all electrides, when the temperature is increased to about 240 K, slow decomposition of the films occurs as indicated by a decrease in the absorbance. We expected that decomposition would decrease the electronic conductivity. Much to our surprise, virtually every run resulted in either an *increase* in

(66) Moeggenborg, K. J.; Papaioannou, J.; Dye, J. L. *Chem. Mater.* **1991**, *3*, 514−520.

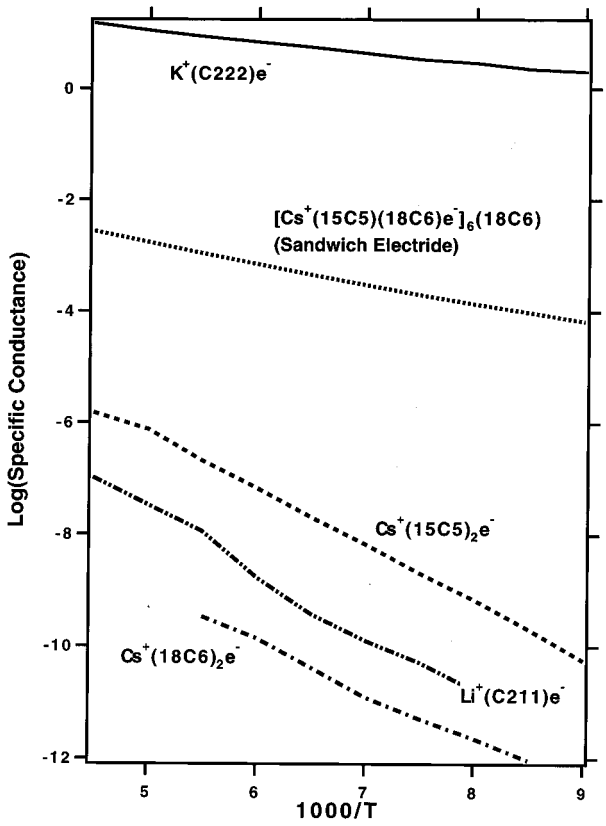

Figure 10. Specific conductances of powdered samples of five electrides as functions of temperature. In most cases the values depend somewhat on the sample, as expected for defect-dominated conductivity.

conductivity or little change, until the decomposition level reached 30−40%, after which the conductivity decreased rapidly to yield an insulting decomposition product.

Although the effect of decomposition could be a surface phenomenon, the relation between film resistance and thickness indicates bulk conductivity, making surface contributions unlikely. The insulating nature of other electrides and the model of electrons trapped in cavities to form Mott insulators suggest that intrinsic electronic conductivity by electron migration and double occupancy of cavities is unlikely. The Coulomb repulsion that would result from such double occupancy is too large to permit rapid electron migration by this mechanism. Thus, we expect a stoichiometric electride to be an insulator. If this is the case, the relatively high conductivity of $K^+(C222)e^-$ must result from the presence of defect electrons or holes that are very mobile.

We propose a model that is consistent with the structure and conductivity behavior of $K^+(C222)e^-$. When either a powdered sample or a film is prepared, some cavities are empty. Empty cavities can be considered as hole defects. The open chain structure of the cavities and channels in $K^+(C222)e^-$ would make such a defect highly mobile along the chain direction. Channel blockage by K^- or structural defects would limit the conductivity, but the interchain channels are large enough to permit activated hopping of defects between chains. The structure suggests that the conductivity should follow a 2D random hopping model. Indeed, the powder conductivity data of Moeggenborg over the temperature range 90−240 K can be fit very well by either a 2D or a 3D random hopping model.[65] The overall behavior could be considered as conduction by *percolation* between highly conducting chain segments *via* the interconnecting channels. The behavior during the early stages of decomposition suggests that additional defects are formed that can compete with blockages resulting from cryptand decomposition. The process is complicated, but the behavior of thin films of $K^+(C222)e^-$, and the variation of conductivity from one electride to another shown in Figure 7 (and also the variation from one preparation to another), suggest strongly that the conductivity of electrides is dominated by mobile defects, either defect electrons or holes.

Summary and Speculation

Electrides are a unique new family of compounds in which there is neither the strong interactions with other electrons and with nuclei that occur with covalent bonds and valence electrons nor the delocalization that is characteristic of metallic electrons. Yet the overall density of electrons is high enough to yield coupling among them. Electrides provide a rich area for theory. Their resemblance to a confined lattice gas of nearly free electrons but with a variety of "plumber's nightmare" geometries should be a challenge to theorists. As a first step, consideration should be given to the relation between interelectron coupling and the length and diameter of connecting channels in a model with simple geometry. Extension of LDA calculations and other *ab initio* methods to the full structure of electrides should also be done.

We have expended considerable effort in attempting to synthesize more crystalline electrides. We have prepared powdered samples of $Rb^+(C222)e^-$, $Na^+(C222)e^-$, $K^+(15C5)_2e^-$, $Rb^+(15C5)_2e^-$, and $Cs^+(C322)e^-$, but so far all attempts to grow single crystals have failed. With the installation of an array-detector X-ray diffractometer at Michigan State University, it is our hope that the structures of the small crystals we see among the powders can be determined.

In principle, there is a virtually unlimited array of complexants that might be used to synthesize new electrides. Collaboration with organic synthesis groups would be very desirable and we welcome such interactions. A problem in such collaborations is our need for gram quantities of complexants to check compatibility with alkali metals, purity, stability, solvent choices, and crystallization methods, etc. However, we are convinced that many additional electrides could be synthesized with the right choices of complexants and metals.

An intriguing new area of study considers the possibility of a continuum between electrides at one extreme and aromatic anions and radical anions at the other. For about four years we have been studying the solution and solid state properties of LOGEAs (large organic globular electron acceptors). These are molecules that contain electron-accepting groups such as aromatic moieties and are large enough to produce cation-trapping voids upon reaction with alkali metals and crystallization. The concept is based on the electron-trapping ability of fullerenes and the formation of fullerides with alkali metals. It would be particularly interesting to develop a "hybrid" in which the voids created by packing were as large as those in electrides, the cations were trapped within the LOGEA, and the electron-accepting groups were marginal in their electron affinity. Such a system might provide an electron density distribution that was spread over both the complexant and the cavity, corresponding to partial occupancy of both types of sites. The optical, magnetic, and electrical properties of such compounds would probably be varied and interesting and perhaps even useful!

Any discussion of electrides with nonchemists always turns to the question of their current or potential usefulness. They and alkali metal anions are already used in organic synthesis[67−74]

(67) Ohsawa, T.; Takagaki, T.; Haneda, A.; Oishi, T. *Tetrahedron Lett.* **1981**, *22*, 2583−2586.

and might be useful in the preparation of nanoscale metal and alloy particles.[75−77] However, their thermal instability is a roadblock to the utilization of their unique electronic properties. We have demonstrated that electride and alkalide powders under some circumstances show thermionic electron emission at temperatures as low as −80 °C.[78] But we do not understand the mechanism, and it appears that the phenomenon does not occur with highly pure samples.[79] We have a far better understanding of photoelectron emission from a sodide and could probably produce an electride-based photoelectron emitter for the near IR region, but it would not be stable for long periods of time. Perhaps the most important aspect of electrides in terms of their usefulness is the demonstration of *potentially* useful properties. Actual applications await the synthesis of more robust electrides, a not impossible task.

Acknowledgment. Research on alkalides and electrides has been supported in part by Grants DMR 87-14751, DMR 90-17292, and 94-02016 from the U.S. National Science Foundation and by annual grants from the Michigan State University Center for Fundamental Materials Research. I am most grateful to the many undergraduates, graduate students, postdocs, and colleagues (named in the references) for their diligent work with electrides in the face of many difficulties and failures. It is to them that I dedicate this paper.

IC970551Z

(68) Ohsawa, T.; Mitsuda, N.; Nezu, J.; Oishi, T. *Tetrahedron Lett.* **1989**, *30*, 845.
(69) Dye, J. L.; Jackson, J. E.; Cauliez, P. In *Organic Synthesis for Materials and Life Sciences*; Yoshida, Z., Ohshiro, Y., Eds.; VCH Publishers: New York, 1992; pp 243−270.
(70) Jedlinski, Z.; Kowalczuk, M.; Grobelny, Z.; Stolarzewicz, A. *R. Macromol. Chem. (London)* **1983**, *4*, 355−358.
(71) Jedlinski, Z.; Kowalczuk, M.; Grobelny, Z.; Stolarzewicz, A. *Macromol. Chem. (London)* **1983**, *4*, 355.
(72) Jedlinski, Z.; Kowalczuk, M.; Kurcok, P. *Makromol. Chem., Macromol. Symp.* **1986**, *3*, 277−293.
(73) Jedlinski, Z.; Kowalczuk, M.; Kurcok, P.; Brzoskowska, L.; Franek, J. *Makromol. Chem.* **1987**, *188*, 1575−1582.
(74) Jedlinski, Z.; Misiolek, A.; Glowkowski, W.; Janeczek, H.; Wolinska, A. *Tetrahedron Lett.* **1990**, *30*, 3547−3558.
(75) Tsai, K. L.; Dye, J. L. *J. Am. Chem. Soc.* **1991**, *113*, 1605−1652.
(76) Tsai, K.; Dye, J. L. *Chem. Mater.* **1993**, *5*, 540−546.
(77) Dye, J. L.; Tsai, K.-L. *Faraday Disc. R. Soc. Chem.* **1991**, *92*, 45−55.
(78) Huang, R. H.; Dye, J. L. *Chem. Phys. Lett.* **1990**, *166*, 133−136.
(79) Kuo, C.; Dye, J. L.; Pratt, W. P., Jr. *J. Phys. Chem.* **1994**, *98*, 13575−13582.